ACS APPLIED MATERIALS & INTERFACES

Research Article

www.acsami.org

Engineering Nanostructures by Decorating Magnetic Nanoparticles onto Graphene Oxide Sheets to Shield Electromagnetic Radiations

Prasanna Kumar S Mural,[†] Shital Patangrao Pawar,[‡] Swetha Jayanthi,[†] Giridhar Madras,[§] Ajay K. Sood,[∥] and Suryasarathi Bose*[,‡]

[†]Center for Nano Science and Engineering, [‡]Department of Materials Engineering, [§]Department of Chemical Engineering, and [∥]Department of Physics, Indian Institute of Science, Bangalore-560012, India

ABSTRACT: In this study, a minimum reflection loss of −70 dB was achieved for a 6 mm thick shield (at 17.1 GHz frequency) employing a unique approach. This was accomplished by engineering nanostructures through decoration of magnetic nanoparticles (nickel, Ni) onto graphene oxide (GO) sheets. Enhanced electromagnetic (EM) shielding was derived by selectively localizing the nanoscopic particles in a specific phase of polyethylene (PE)/poly(ethylene oxide) (PEO) blends. By introduction of a conducting inclusion (like multiwall carbon nanotubes, MWNTs) together with the engineered nanostructures (nickel-decorated GO, GO-Ni), the shielding efficiency can be enhanced significantly in contrast to physically mixing the particles in the blends. For instance, the composites showed a shielding efficiency >25 dB for a combination of MWNTs (3 wt %) and Ni nanoparticles (52 wt %) in PE/PEO blends. However, similar shielding effectiveness could be achieved for a combination of MWNTs (3 wt %) and 10 vol % of GO-Ni where in the effective concentration of Ni was only 19 wt %. The GO-Ni sheets facilitated in an efficient charge transfer as manifested from high electrical conductivity in the blends besides enhancing the permeability in the blends. It is envisioned that GO is simultaneously reduced in the process of synthesizing GO-Ni, and this facilitated in efficient charge transfer between the neighboring CNTs. More interestingly, the blends with MWNTs/GO-Ni attenuated the incoming EM radiation mostly by absorption. This study opens new avenues in designing polyolefin-based lightweight shielding materials by engineering nanostructures for numerous applications.

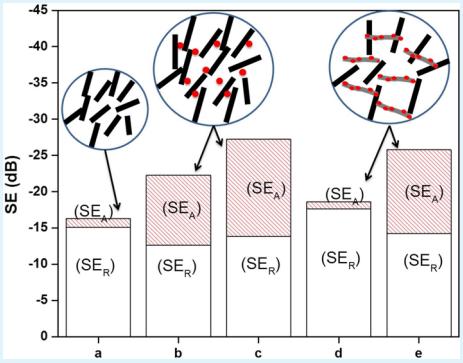

KEYWORDS: *MWNT, PE/PEO blends, nickel nanoparticles, graphene oxide, EMI shielding*

INTRODUCTION

Because of electromagnetic radiations emitted by electronic gadgets, electromagnetic interference (EMI) is a major concern in the current era. In addition to interfering with the precise electronic circuitry, they also pose several health issues.[1−3] Thus, there is an urgent need to develop materials that can block these EM radiations. Though EM radiations can be attenuated by reflecting or absorbing the incoming radiations, the latter is more desirable for many applications.[2] Metals are the primary choice for shielding, but they suffer from certain limitations such as difficulties in processability, structural flexibility and environmental stability.[4−9] However, these difficulties can be overcome by using polymeric composites because of their excellent processability, flexibility, and tailor-made properties.[7]

Polymeric materials are insulators, inherently nonmagnetic, and thus are transparent to these radiations. In this context, incorporation of conducting inclusions and magnetic nanomaterials can shield the incoming radiations. For high electrical conductivity, multiwall carbon nanotubes (MWNTs) is an ideal choice because of their high aspect ratio that lowers their percolation threshold in contrast to metal nanoparticles.[10] However, the lack of magnetic dipoles restricts their application in shielding by absorption. In this context, ferromagnetic materials like iron (Fe), cobalt (Co), and nickel (Ni) can be promising materials for shielding EM radiations. They can be introduced either by decorating or by physical mixing with CNTs. The latter in general is preferred because decoration of CNTs with metal nanoparticles often results in defects, which in turn lead to deterioration of electrical properties of CNTs and, hence, might affect the overall shielding efficiency. Furthermore, the size of these decorated magnetic nanoparticles is usually small and their effect on EM absorption is weaker. In addition, although the basic mechanism of shielding in these ferromagnetic materials is by absorption but it is realized only at higher loadings.[7]

Polymer blends are a class of materials that possess superior properties than their components and are also versatile in context to ecological and economical viewpoint.[11] Polymer blends have widespread use and can replace traditional materials, such as metals, for many functional applications.[12] In addition, the percolation threshold of conducting nanoparticles can be reduced significantly by selectively filling one of the phases of the blends.[13−15] This increases the local

Received: March 28, 2015
Accepted: July 15, 2015
Published: July 15, 2015

DOI: 10.1021/acsami.5b02703
ACS Appl. Mater. Interfaces 2015, 7, 16266−16278

concentration of the nanoparticles resulting in more interconnections. For instance, the percolation threshold of MWNTs was reduced significantly in immiscible blends of PE and PMMA with respect to their components.[14] In the recent past, several studies have reported enhanced shielding efficiency in MWNTs based polymeric composites. For instance, Singh et al.,[16] reported a shielding effectiveness of −22 dB was reported in LDPE (low density polyethylene) composites with 10 wt % MWNTs. Similarly Al-Saleh et al.,[17] reported that incorporation of 7.5 vol % MWNT in polypropylene (PP) exhibited a shielding effectiveness of 35 dB. In the case of polystyrene (PS) with 7 wt % MWNTs, an shielding effectiveness of 20 dB was reported by Yang et al.[18] Further, Hoang et al.,[19] reported that with the addition of 25 wt % MWNTs in polyurethane, the shielding effectiveness of 25 dB can be obtained. With the addition of 15 wt % SWNTs in epoxy matrix, Huang[20] reported a shielding effectiveness of 20−30 dB EMI SE in the X-band range. Liang et al.[21] also reported that 15 wt % of graphene sheets in epoxy matrix exhibit a shielding effectiveness of 21 dB. EMI shielding effectiveness was tested over a frequency range of 8.2−12.4 GHz (X-band), and 21 dB shielding efficiency was obtained for 15 wt % (8.8 vol %) loading, indicating that they may be used as lightweight, effective EMI shielding materials. Maiti et al.,[22] reported a shielding effectiveness of 23 dB in polycarbonate (PC) with the addition of 2 wt % MWNT.PMMA with addition of 40 wt % MWNTs exhibited a shielding effectiveness of 27 dB.[23] Recently, Kar et al.,[24] reported a high shielding effectiveness of 23 dB with very low fraction of MWNTs in PVDF. Further, Zhang et al.[25] reported that ultralight and highly compressible graphene foams exhibit a 3D conductive network which plays a vital role in resulting in EM absorption as high as 2.2×10^5 dB cm^2 g^{-1}. It is well evident from the above literature that high shielding effectiveness can be obtained at relatively higher fraction of conducting nanoparticles. However; the structural properties can deteriorate at such high loadings. Hence, a great deal of research is being focused toward developing EMI shielding materials with low amounts of functional nanoparticles in order to design lightweight and flexible shields.

It is well reported that the material should possess both electric and/or magnetic dipoles, which interact with the electromagnetic field and block the incoming radiation. Thus, incorporation of nanoparticles like Fe (iron), Ni (nickel), Co (cobalt), etc., along with MWNTs can further enhance the shielding. For instance, Kar et al.,[24] reported that incorporation of Fe_3O_4 along with MWNTs (modified with ionic liquid) in PVDF/ABS led to significant enhancement in the shielding effectiveness. Similarly, Pawar et al.,[7] developed Fe_3O_4 magnetic nanoparticles grafted MWNTs that exhibited shielding effectiveness of 28 dB in PC/SAN blends. In this context, Ni is preferred over Co or Fe because of its superior oxidative resistance[26]

In the development of conducting polymer nanocomposites, high aspect ratio nanoparticles are ideal candidates as they manifest in low geometrical percolation threshold. Thus, MWNT and graphene are promising materials to design and develop conducting polymer nanocomposites. MWNT possess high intrinsic conductivity whereas graphene oxide exhibits high dielectric constant because of charge accumulation on account of oxygen moieties on the basal plane of graphene. To attenuate electromagnetic (EM) radiation, materials should preferably possess electrical conductivity, dielectric, and magnetic dipoles. However, MWNT and graphene oxide are nonmagnetic and thus are transparent to magnetic field associated with EM radiations. Hence, various approaches have been designed to incorporate magnetic materials along with conducting nanoparticles for developing EMI shielding materials. However, incorporation of magnetic nanoparticles can lead to agglomeration in the polymer matrix. Interestingly, by nucleating magnetic nanoparticles on the graphene sheet, the quality of dispersion can be improved to a significant extent. Thus, in the present study, a unique approach has been adopted to block EM radiation by absorption through synergistic effects from GO, Ni, and MWNTs in a techno-commercial blend like PE and PEO.

The rationale behind this work is to reduce the concentration of nanoparticles required to achieve efficient shielding of EM radiations. This will help in the design of polymer based lightweight and flexible shielding materials. The blends of PE and PEO were chosen because of their ease of processing, chemical inertness, and low density. Various strategies were adopted like physical mixing the magnetic nanoparticles along with conducting inclusions (MWNTs), decorating magnetic nanoparticles on MWNTs and graphene oxide (GO) sheets, etc. The engineered nanostructures were observed to be more efficient when compared to physical mixing both the entities in the blends. By selectively localizing the nanostructures in the PE phase, an efficient charge transport was facilitated, as manifested from electrical measurements. The nanostructures were well-characterized using microscopic and spectroscopic techniques. The EM shielding parameters were assessed using a vector network analyzer coupled to a coaxial set up in a broad frequency range encompassing both X and K_u-band.

EXPERIMENTAL SECTION

Materials. PE (low density polyethylene with MFI of 25 g/10 min), PEO (poly(ethylene oxide) M_V of 400 000 g/mol), and nickel chloride hexahydrate ($NiCl_2{\cdot}6H_2O$) were procured from Sigma-Aldrich. The multiwalled carbon nanotubes (MWNT) with ∼1.5 μm long and 9.5 nm average diameter (NC 7000 of 90% purity) were obtained from Nanocyl (Belgium). Acrylic acid was procured from Alfa Aesar (Germany). All other solvents and reagents of analytical grade were procured from SD. Fine chemicals (India) and used without any further modification.

Synthesis of Graphene Oxide (GO). GO was synthesized as described in our previous work.[27] Briefly, graphitic flakes were oxidized with $KMnO_4$ in the presence of H_2SO_4 and H_3PO_4 (9:1 v/v), and the mixture was kept at room temperature. After 72 h, oxidation was stopped by the addition of hydrogen peroxide. The mixture was then filtered and washed with distilled water, hydrochloric acid and ethanol was added successively. Thus, the obtained GO lumps were vacuum-dried at room temperature.

Synthesis of Ni Nanoparticles Decorated MWNTs and GO Sheets. Ni-decorated MWNTs were synthesized by grafting PAA onto MWNT and the carboxyl moieties were utilized for the attachment of Ni particle as described elsewhere in the literature.[28] MWNT-Ni and GO-Ni were prepared by reducing $NiCl_2{\cdot}6H_2O$ salt on to PAA-MWNT and GO using hydrazine hydrate as the reducing agent and in the presence of sodium hydroxide as a catalyst in ethylene glycol (EG).[28] Briefly, 30 mg of PAA-MWNT or GO was sonicated in 50 mL of EG, along with 62 mg of $NiCl_2{\cdot}6H_2O$ and 0.26 g of NaOH as catalyst. Then the reaction mixture was kept at 80 °C for 2 h, washed and centrifuged with DI water (5 times). To synthesize Ni nanoparticles, all the steps mentioned above were followed without the PAA-MWNT and GO sheets.

Preparation of Blend Nanocomposites. PE (70 wt %) and 30 wt % PEO blends with MWNTs, Ni, and GO-Ni were melt mixed in a twin screw extruder (Thermo Haake Minilab II) at 150 °C and 60 rpm for 20 min under N_2 atmosphere. The recirculation channel ensured

DOI: 10.1021/acsami.5b02703
ACS Appl. Mater. Interfaces 2015, 7, 16266−16278

Scheme 1. Ni Decoration on the Surface of MWNT

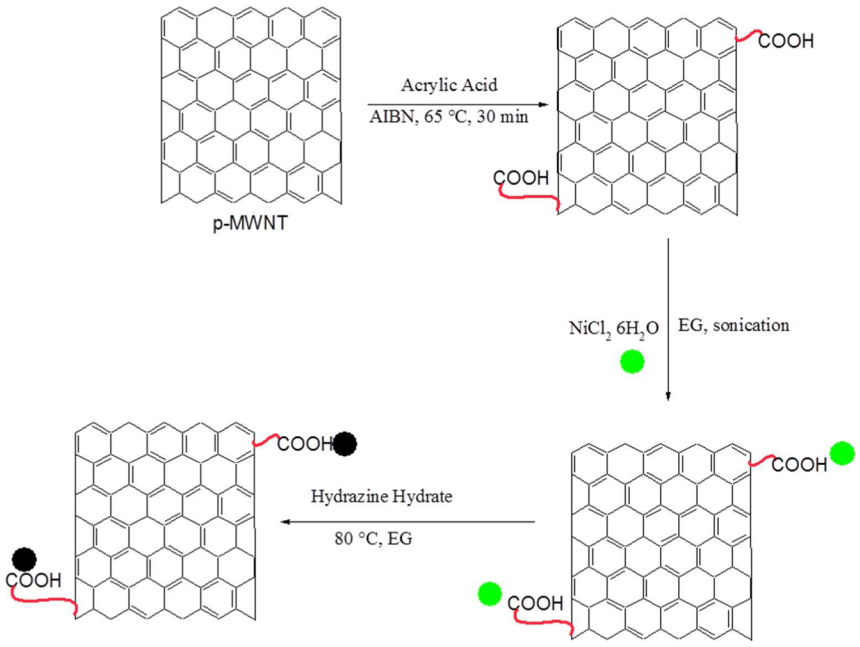

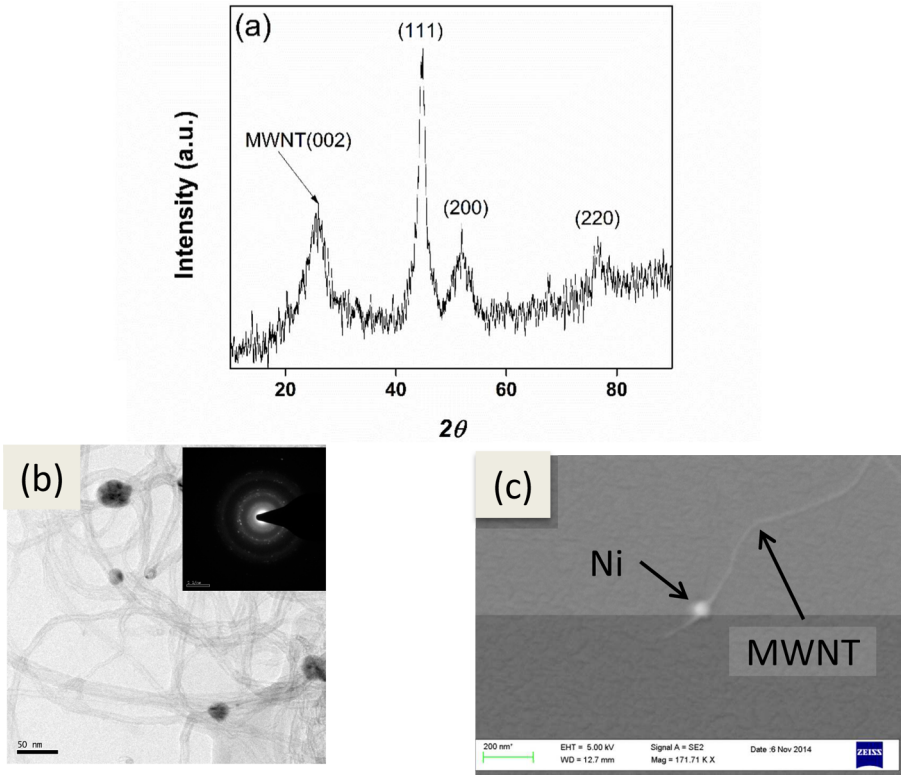

Figure 1. (a) XRD pattern, (b) TEM (inset shows the diffraction pattern), and (c) SEM micrograph of Ni-MWNT.

homogeneous mixing of particles in the blend. Prior to melt mixing, PE and PEO was vacuum-dried to remove traces of moisture.

Characterization of Nanoparticles and Blend Nanocomposites. The size and morphology of the nanostructures were analyzed by transmission electron microscopy (TEM), using a Tecnai G2T20, and field emission scanning electron microscopy (FESEM) using ULTRA 55 from Carl Zeiss. The various functional groups on the nanostructures were assessed using Fourier transform infrared (FTIR) from PerkinElmer Frontier. The crystal structure was evaluated by X-ray diffraction (XRD) using a Cu K_α source. The magnetic properties were evaluated using a Vibratory Sample Magnetometer (VSM) (from Lakeshore) at room temperature with an applied field of −2000 to 2000 Oe. The phase morphology of the extruded strands was studied using SEM. To enhance the contrast, the PEO phase was etched using cold water.

AC electrical conductivity of the various blend nanocomposites were studied using an Alpha-N Analyzer, Novocontrol with the frequency range from 10^{-1} to 10^{7} Hz. The electromagnetic interference (EMI) shielding effectiveness (SE) was measured in the frequency range of 2−18 GHz. Specimens for EMI SE measurement

DOI: 10.1021/acsami.5b02703
ACS Appl. Mater. Interfaces 2015, 7, 16266−16278

were prepared using compression molding. The various EMI shielding parameters was evaluated using Anritsu MSA4642A, two port vector network analyzer (VNA) coupled with a coaxial setup (from Damaskos). Prior to the measurements, absorption and reflection losses arising due to the transmission line and sample holder were avoided by full SOLT calibration through two ports.

RESULTS AND DISCUSSION

Synthesis and Characterization of Ni Nanoparticles and Ni-Decorated MWNT and GO. Among the various strategies for decorating nickel (Ni) on MWNTs like immersion of MWNTs in salt solution, heat treating the coated MWNTs under H_2 atmosphere,[29] electro-evaporation of Ni in MWNT dispersed solution,[30] etc., chemical reduction of Ni salt on MWNTs is the most efficient, simple, versatile, and easily scalable.[31] Ni decoration on to MWNTs is governed by many functional groups present on the surface of MWNTs. Out of the various functional groups, the carboxylic groups are commonly utilized for decorating Ni nanoparticles.[32,33] The carboxylic functional groups can be introduced via oxidation of the surface of MWNTs.[34,35] However, oxidation of MWNTs results in defects.[36] In the present work, acrylic acid was in situ polymerized in the presence of MWNTs which results in the introduction of many carboxyl groups on the surface of MWNTs, as shown in Scheme 1 Further, carboxylic groups thus introduced on the surface were utilized for nucleation of Ni during chemical reduction using hydrazine hydrate. The reduction of $NiCl_2{\cdot}6H_2O$ on the surface was further confirmed by XRD (see Figure 1).

In Figure 1a, the peaks corresponding to 2θ of 44, 51, and 76 (JCPDS card no. 00-001-1258) are attributed to [111], [200], and [220] crystal planes of cubic Ni.[37] This further supports that Ni is in pure metallic state. The graphitic peak corresponding to (002) reflection is observed at 2θ = 26.4°. But in case of MWNTs, a downward shift at 2θ = 25.9° is noted and is attributed to sp^2, C═C layers spacing.[38] Park et al.[39] reported that decoration of silver on the MWNT showed a 2θ = 25.9° along with silver peaks at 38.0°, 44.4°, 64.5°, and 77.5° that suggests the presence of MWNT along with silver. Similarly, in our study, we observed the MWNT peak at 2θ = 25.51° along with 2θ = 44.5°, 51.8°, and 74.4° that can be assigned to (111), (200), and (220) (2θ) reflection of face-centered cubic Ni crystals suggesting the presence of MWNT, along with nickel.

TEM micrograph (Figure 1b) suggests Ni nanoparticles of ~49 nm are decorated on the surface of MWNTs. The inset in Figure 1b shows the selected area electron diffraction (SAED) of Ni, which exhibits a symmetrical dotted lattice of Ni. SEM micrograph of Ni-MWNT (Figure 1c) shows distribution of Ni on the surface of MWNTs.

Similarly, Ni was decorated on the surface of GO, which was synthesized by oxidation of graphite by Hummers method,[40] as shown in Scheme 2. From Figure 2i, it is evident that upon oxidation of graphite, the carboxyl (1710 cm^{-1}), epoxy (1050 cm^{-1}), and hydroxyl groups(broad peak at 3300 cm^{-1}) are introduced on to the surface of GO. Ni was decorated on the surface of GO by in situ reduction of $NiCl_2$using hydrazine hydrate in the presence of NaOH. However, during this process GO undergoes partial reduction, as revealed from FTIR. From Figure 2i, it is evident that the absence of carboxyl and reduction of hydroxyl peak suggest partial reduction of GO during the synthesis of GO-Ni.

Scheme 2. Synthesis of Ni-Decorated GO Sheets

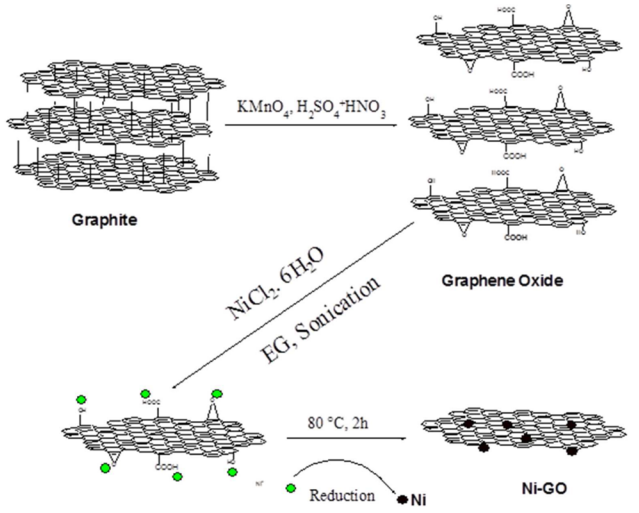

It is evident from Figure 2ii(b) that Ni is uniformly distributed on the surface of GO sheets. Metal ions carry a positive charge and tend to get stabilized in the presence of negatively charged GO sheets[41] during sonication. Further, hydrazine hydrate, a reducing agent is utilized for reduction of these stabilized Ni ions to metallic Ni. This reduction at specific sites prevents agglomeration of Ni nanoparticles on the surface of GO sheets. In addition, attachment of Ni nanoparticles hinders the restacking of GO sheets. From Figure 2ii(a), it is evident that Ni nanoparticles prepared under identical experimental conditions tend to agglomerate to form large particles. Hence, GO sheets tend to efficiently support the growth and distribution of Ni particles on the surface because of its large surface area.

TEM micrograph of Ni (Figure 2iii(a)) suggests agglomeration of Ni particles with an average size of 150−200 nm. The TEM micrograph of GO-Ni (Figure 2iii(b)) showed that Ni particles of 6−15 nm are uniformly distributed on the GO sheets, which is due to interaction of GO sheets with Ni ions. Similar observations have been reported earlier.[42]

Figure 2iv shows the XRD pattern of Ni nanoparticles and GO-Ni and it is evident that both Ni and GO-Ni exhibit characteristic peaks at 44°, 51°,and 76° that can be attributed to [111], [200], and [222] crystal planes of cubic structure of Ni (JCPDS card no. 00-001-1258). The broadening of peak at 24° suggests the reduction of GO sheets, as shown in the inset of Figure 5. Further, XRD supports the observations made from XPS, as shown in Figure 2v. From XPS, the peaks corresponding to $2p_{3/2}$ and $2p_{1/2}$ spin states of Ni are evident at binding energies of 855 and 873 eV, respectively. Quantitative elemental analysis manifested 44% (atomic %) of nickel.

Electrical Conductivity. It is reported that the selective localization of conducting filler in one phase of blend can lead to synergistic improvement in the conductivity.[43] This synergism in the improvement of conductivity is attributed to effective increase in concentration of filler in a given phase and usually observed in cocontinuous type of microstructures. However, in case of PE/PEO blends, more the PEO, poorer is the structural properties of the blends. This infers that high concentration of PEO will limit its use for structural applications. Hence, we vary the concentration of PEO in the

DOI: 10.1021/acsami.5b02703
ACS Appl. Mater. Interfaces 2015, 7, 16266−16278

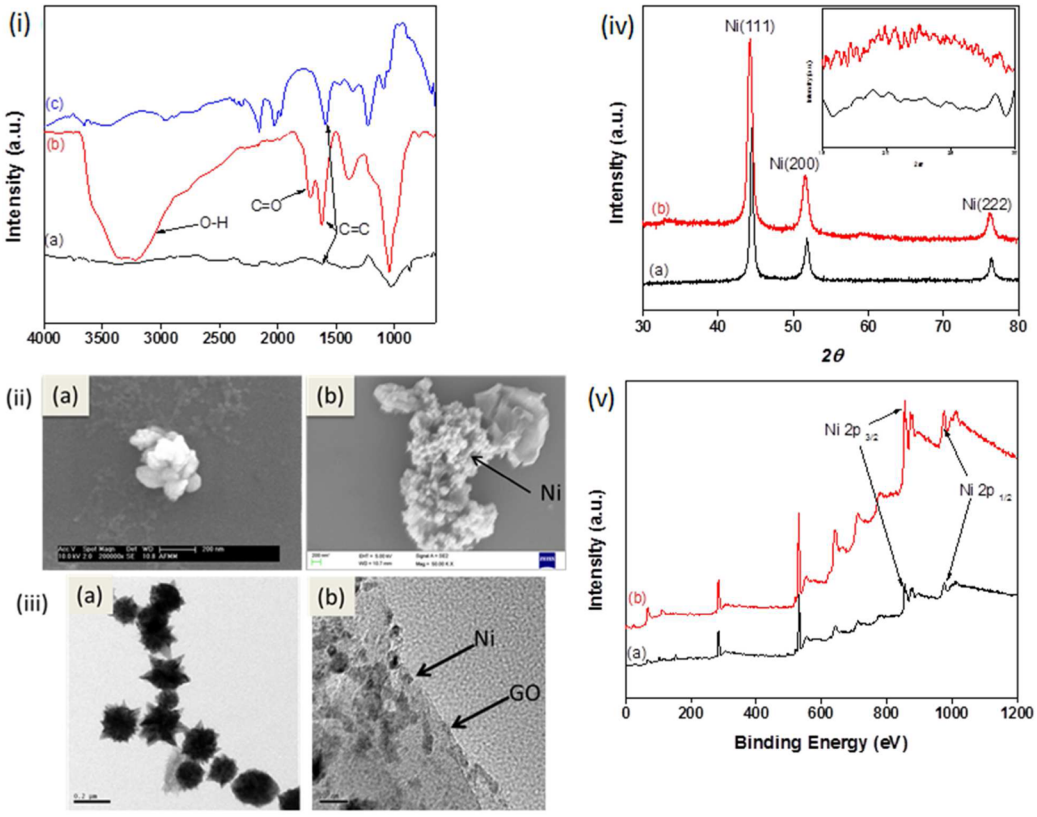

Figure 2. (i) FTIR spectra of (a) graphite, (b) GO, and (c) GO-Ni. (ii) SEM micrograph of (a) Ni and (b) GO-Ni. (iii) TEM micrograph of (a) graphite and (b) GO. (iv) XRD pattern of Ni and GO-Ni (inset shows rGO broad peak at 24°). (v) XPS spectrum of (a) Ni and (b) GO-Ni.

blends from 10−50 wt % and evaluated the bulk electrical conductivity with 1 wt % MWNTs.

As shown in Figure 3, the concentration of PEO (dispersed phase) was varied between 10−50 wt % in PE matrix with 1 wt

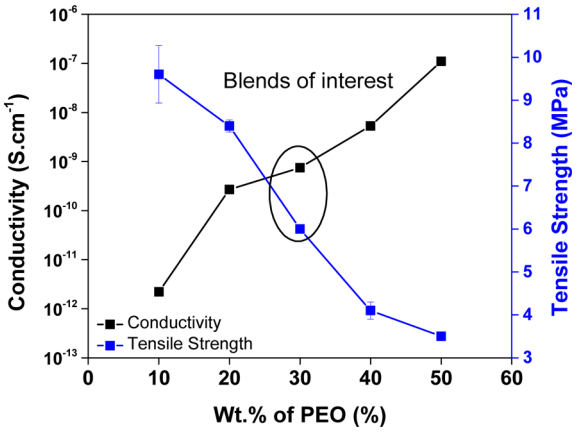

Figure 3. AC conductivity at 1 Hz and tensile strength of PE/PEO blends with varying PEO concentration (the lines are only intended to guide the eye).

% MWNT (for conductivity). It is observed that the composite with 50 wt % PEO exhibited a conductivity of $\sim 10^{-7}$ S·cm^{-1} however resulted in poor mechanical properties. This reduction in mechanical properties (tensile strength) with increase in PEO (dispersed) content suggests a negative deviation from mixing rule.[44] This indicates a poor adhesion at the interface because of phase separation of PEO in PE phase. The lower PEO content leads to a decrease in electrical conductivity (as 10 wt % PEO exhibit conductivity of 10^{-12} S·cm^{-1}). Hence, for further studies, the composite with 30 wt % PEO and 70 wt % PE was chosen from practical viewpoint, which exhibit a good set of electrical and mechanical properties.

The electrical conductivities of 70/30 wt./wt. PE/PEO blends with 1−3 wt % MWNTs and Ni-MWNT and PAA-*g*-MWNT were assessed at room temperature by broadband dielectric spectroscopy from 10^{-1} Hz to 10^{-7} Hz. It is evident from Figure 4a that with an increase in MWNT concentration, electrical conductivity increases. Further, addition of 3 wt % of MWNT exhibited a conductivity of 10^{-6} S.cm^{-1}, an increase of 7 orders of conductivity with respect to neat blends. This increase in conductivity is attributed to transport of electrons through 3D network. In the present work, MWNTs are restricted in the PE phase, as reported in our earlier work.[14] Further, it is worth noting that the percolation concentration in PE matrix reported in 3.6 vol % (~6 wt %).[45] The effect of selective localization is evident in PE/PEO (70/30 wt./wt.) blend wherein percolation of MWNTs is achieved at 3 wt %. Thus, further studies were restricted to 3 wt % MWNT in (70/30) PE/PEO blend.

Further, to achieve high EMI shielding, high electrical conductivity and magnetic properties are desired. To our surprise, the PE/PEO blends with 3 wt % of Ni-MWNT nanoparticles exhibited a conductivity, which is 4 orders lower than MWNT. This contradicts the observation made by Ryu et al.,[46] who reported that Ni decorated CNT showed one order increase in conductivity in contrast to pristine CNTs in epoxy matrix. In order to understand this phenomena, 3 wt % PAA-*g*-MWNT were mixed with PE/PEO blends. The PAA-*g*-MWNT

DOI: 10.1021/acsami.5b02703
ACS Appl. Mater. Interfaces 2015, 7, 16266−16278

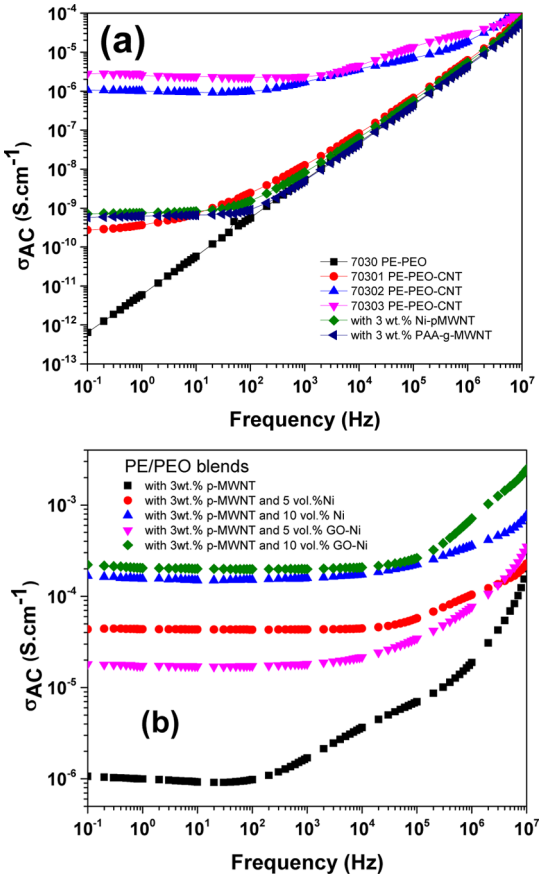

Figure 4. (a) AC conductivity of 70/30 PE/PEO neat, with 1−3 wt % of MWNT, with 3 wt % Ni-MWNT and with 3 wt % PAA-*g*-MWNT, and (b) conductivity of 70/30 PE/PEO blends.

also exhibited conductivity in the range of 10^{-10} S cm^{-1} similar to Ni-MWNT. Hence, we attribute the drop in conductivity due to wrapping of PAA on the surface of MWNT. Therefore, Ni-MWNT may be not be a good candidate as a shielding material. Hence, for our further studies, we have used Ni and GO-Ni in PE/PEO along with MWNT.

Blends with Ni and GO-Ni were assessed through electrical conductivity where MWNT concentration (3 wt %) was kept constant (Figure 4b). Addition of Ni and GO-Ni both manifested enhanced electrical conductivity over blends with 3 wt % MWNTs. Interestingly, blends with 10 vol % of Ni (52 wt %) and GO-Ni (19 wt %) manifested similar electrical conductivity though weight fraction of GO-Ni is strikingly smaller over Ni nanoparticles. Blends with 10 vol % GO-Ni along with 3 wt % MWNTs manifested highest electrical conductivity of 2×10^{-4} S/cm. These observations suggest that approach of decoration of GO sheets with Ni nanoparticles resulted in enhanced conductivity at very small fraction of filler loading. Further incorporation of Ni and GO-Ni exhibited synergetic effect on conductivity due to the conducting path provided by nanoparticles.

Magnetization of GO-Ni and Ni Nanoparticles. It is well reported that magnetic dipoles play a vital role in the attenuation of EM radiation.[7] Thus, the magnetic properties of the Ni and GO-Ni nanoparticles were determined at room temperature. The magnetization curve of MWNT (depicted in Figure 5a) exhibited a negligible magnetization value of 0.3 emu g^{-1} which can be attributed to the residual metal catalyst present during the synthesis. Further from Figure 5b it evident that both Ni and GO-Ni nanoparticles exhibited a ferromagnetic behavior, with a saturation magnetization of 56.9 and 23.4 emu g^{-1} respectively. Various magnetization values are listed in Table 1. The remnant magnetization (M_r) of Ni is 21.4 and the

Table 1. Magnetization Values of Ni, GO-Ni, and MWNT

particle	M_s (emu·g^{-1})	M_r (emu·g^{-1})	H_c (Oe)	M_r/M_s
Ni	56.9	21.4	257	0.37
GO-Ni	23.4	8.9	312	0.38
MWNT	0.3	0.2	250	0.67

saturation magnetization (M_s) of Ni is 56.9 emu g^{-1}, which is similar to the earlier reported magnetization values.[47] Ni has multiple crystal domains that result in the enhancement[35] of the effective magnetic moment. Further, GO-Ni showed remnant magnetization (M_r) of 8.9 and saturation magnetization (M_s) of 23.4 emu g^{-1}. This decrease in saturation magnetization is attributed to presence of relatively non-magnetic GO sheets.

The coercivity (H_c) is an ability of material to withstand external magnetic field without getting demagnetize. The coercivity (H_c) is dependent on the shape and crystallite size of material, nature of the boundaries, and also the surface and initial layer properties. The coercivity (H_c) of Ni is 257 and GO-Ni to be 312 Oe, as shown in Figure 5 inset. This increase in H_c is attributed to smaller Ni particles present on the surface thus resulting in magnetization reversal to withstand an external

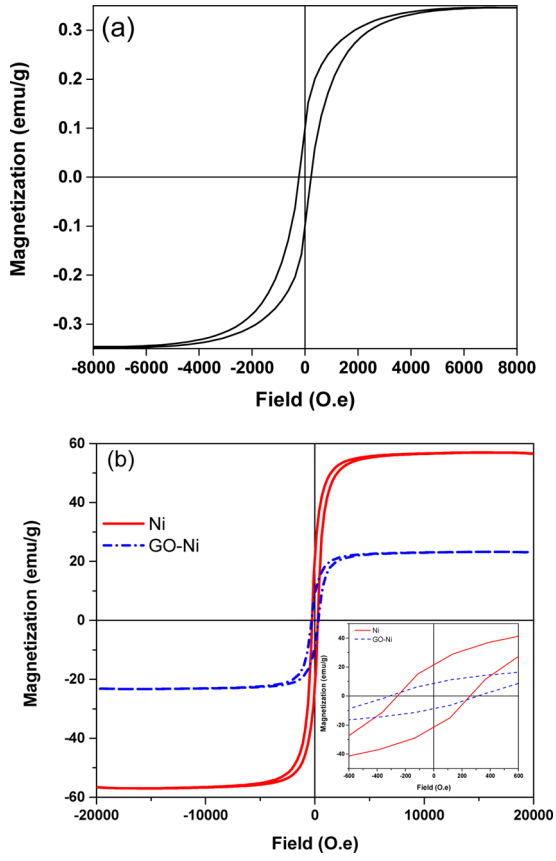

Figure 5. Magnetic hysteresis loops of (a) MWNT and (b) Ni and GO-Ni versus magnetic field at room temperature (inset shows the zoomed magnetic hysteresis loops of Ni and GO-Ni versus magnetic field).

DOI: 10.1021/acsami.5b02703
ACS Appl. Mater. Interfaces 2015, 7, 16266−16278

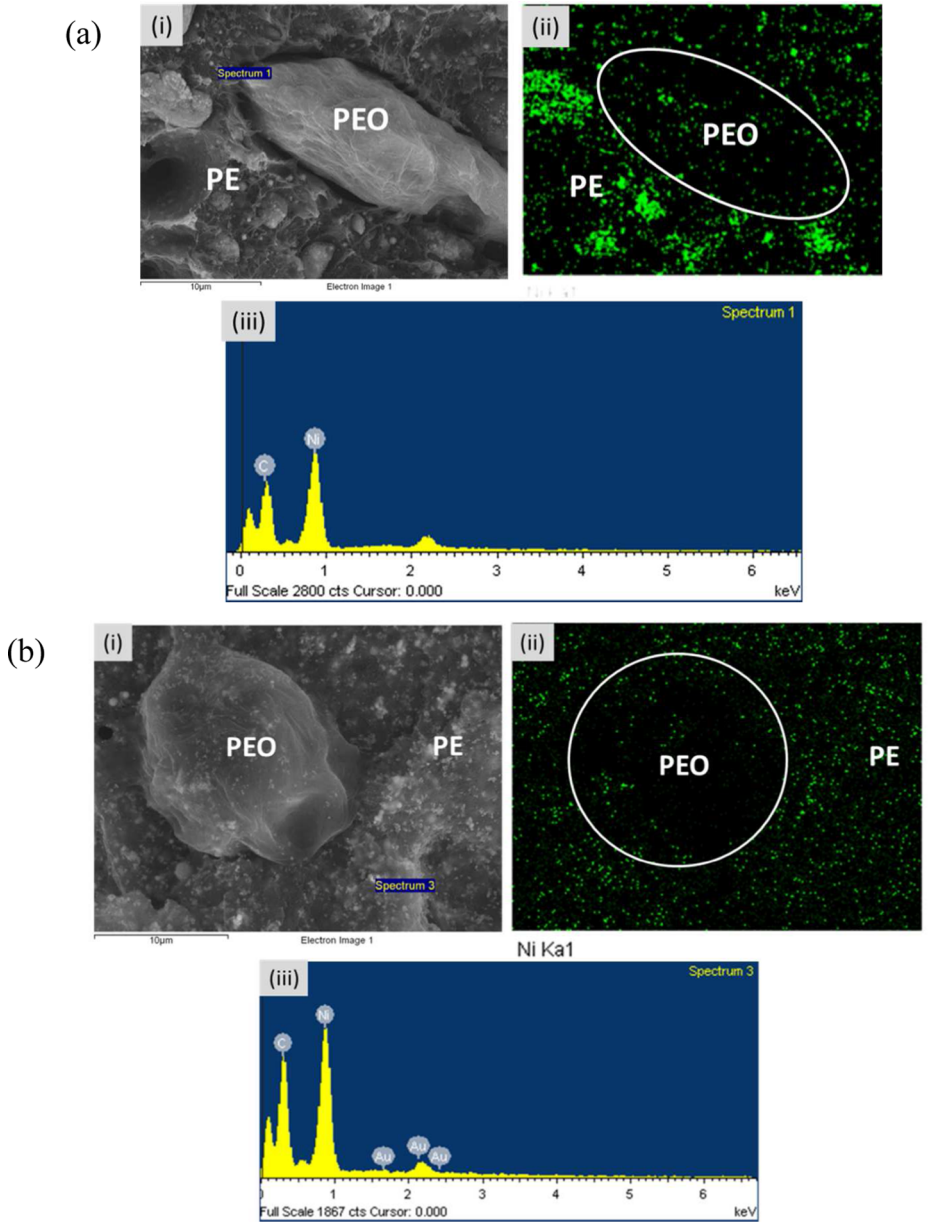

Figure 6. Morphology and EDAX mapping of 70/30 PE/PEO without etching PEO with 3 wt % MWNT and 10 vol % Ni is shown in panel a and with 3 wt % MWNT and 10 vol % GO-Ni is shown in panel b: (i) blend morphology, (ii) one-to-one Ni mapping, and (iii) EDAX spectrum.

magnetic field without becoming demagnetized. This higher H_c in case of GO-Ni nanoparticles can further leads to enhanced absorption of magnetic field associated with EM radiation through hysteresis magnetic losses.

Blend Morphology. The morphology of cryo-fractured 70/30 wt./wt. PE/PEO blends with 3 wt % of MWNT, with Ni nanoparticle and GO-Ni was analyzed by FESEM. PE/PEO exhibited typical sea−island type of morphology with PEO dispersed uniformly in PE. Figure 6a shows the morphology (i) of PE/PEO with 10 vol % Ni and Figure 6a (ii) illustrates the Ni mapping. It is evident from EDAX mapping that Ni is mostly localized in the PE phase. It is interesting to note from Figure 6a (ii) that Ni nanoparticles are mostly agglomerated in the PE phase. This is attributed to strong van der Waals' force between the Ni nanoparticles. Similarly, Figure 6b reflects the morphology of PE/PEO blends with 10 vol % GO-Ni and the corresponding EDAX mapping, as shown in Figure 6b (ii), illustrates the localization of GO-Ni in the PE phase. It is interesting to note that unlike Ni nanoparticles, the GO-Ni nanoparticles are uniformly distributed in the PE matrix. Thus, decoration of Ni nanoparticles on the GO sheet facilitates in efficient dispersion of GO sheets in the blends.

Attenuation of EM Radiations. The attenuation of electromagnetic (EM) radiation was measured using scattering parameter and expressed as shielding effectiveness (SE). From basic phenomenon of EMI shielding, it is well-known that electrically conducting materials are good for EMI shields. Apart from electrical conductivity, magnetic dipoles also play a vital role in attenuating the incident EM radiations.[23,48] The shields are considered to be exhibited by three main mechanisms, that is, reflection (SE_R), absorption (SE_A), and internal multiple reflection (SE_{MR}). SE_R is exhibited by materials containing free electron or mobile charge carrier. SE_A is exhibited by materials with electrical and magnetic

DOI: 10.1021/acsami.5b02703
ACS Appl. Mater. Interfaces 2015, 7, 16266−16278

dipoles. SE_{MR} occurs due to reflections across the internal surfaces. EMI SE total (SE_T) is expressed as

$$SE_T = SE_R + SE_A + SE_{MR} \quad (1)$$

SE_T of materials can be calculated by using the scattering parameter as

$$SE_T\,(dB) = 10 \times \log\left[\frac{1}{|S_{12}|^2}\right] = 10 \times \log\left[\frac{1}{|S_{21}|^2}\right] \quad (2)$$

In eq 2, S_{12} and S_{21} correspond to reverse transmission coefficient and forward transmission coefficient, respectively.

From literature, it is clear that the conductivity and connectivity of MWNT plays a vital role in achieving the high attenuation of EM radiation. The present work focuses on establishing MWNTs network by selectively localizing them in the PE phase. Further partial/unconnected MWNTs are bridged by Ni nanoparticles/GO-Ni. This connectivity results in the increase of conductivity, as discussed earlier.

Figure 7 exhibits the total shielding effectiveness (SE_T) (with specimen thickness of 6 mm) as a function of frequency for

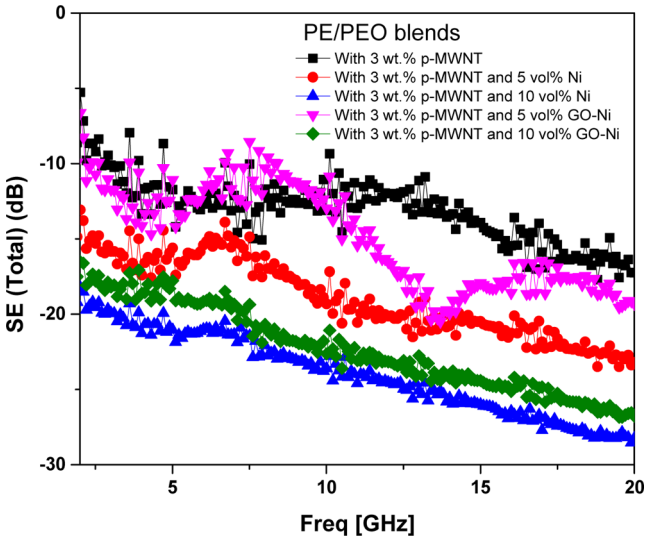

Figure 7. Total shielding effectiveness as a function of frequency for 70/30 PE/PEO with 3 wt % MWNT and 5−10 vol % Ni and GO-Ni (with specimen thickness of 6 mm).

different blends studied here. The blends with 3 wt % MWNTs manifested a total shielding effectiveness of −16.3 dB at 18 GHz frequency. Whereas, addition of Ni and GO-Ni nanoparticles, resulted in enhanced total SE. Thus, addition of 5 (10 wt %) and 10 vol % (19 wt %) GO-Ni manifested a SE_T of −18 and −26 dB, respectively. This observation can also be easily correlated with electrical conductivity where addition of Ni and GO-Ni led to increase in conductivity. Furthermore, total SE was scaled with fraction of Ni and GO-Ni nanoparticles. In case of blends with 5 vol % (34 wt %) Ni nanoparticles, SE was significantly enhanced to −23.4 dB over the blends with only 3 wt % MWNTs (−17 dB) whereas for blends with 5 vol % (10 wt %) GO-Ni manifested only a small increment in the SE total to −19 dB at 18 GHz frequency. This could be due to relatively low weight fraction of GO-Ni nanoparticles were not enough to form connecting network. Surprisingly, at higher fraction (10 vol %), though relative weight fraction of GO-Ni (19 wt %) is very small over Ni nanoparticles (54 wt %), total shielding effectiveness was observed to be comparable in both the blends. This may ascribed to effective network formation of MWNTs and Ni nanoparticles decorated on graphene oxide sheets. It is well understood that network of fillers leads to enhancement in EM attenuation.

In case of polymer nanocomposites containing conducting fillers, the connecting network can be assessed through electrical conductivity measurements. Figure 4b shows that the blend with 3 wt % MWNTs and 5 vol % Ni manifested higher electrical conductivity in contrast to the blend with 3 wt % MWNTs and 5 vol % GO-Ni. Moreover, further addition of GO-Ni (10 vol %) resulted in strikingly enhanced electrical conductivity. From electrical analysis, it is evident that the blends with 3 wt % MWNTs and 5 vol % GO-Ni lack interconnections between the conducting inclusions. However, 10 vol % GO-Ni manifested in a connecting network that further led to an enhanced EM attenuation.

From EMI shielding analysis, it is clear that dispersion and connecting network of nanofillers plays a prominent role in EMI attenuation. In case of blends with MWNTs and Ni nanoparticles, owing to their magnetic nature of Ni nanoparticles, this led to agglomeration in polymer matrix and fraction required to form connecting network of filler was observed to be relatively very high over GO-Ni nanoparticles. The GO-Ni nanoparticles manifested comparative EMI shielding attenuation to physically mixed Ni nanoparticles at very low weight fraction of nanoparticles. Owing to their high surface area, GO nanosheets acted as an effective substrate to decorate Ni nanoparticles and assisted in effective dispersion and network formation. These observations manifests that strategy of uniform decoration of magnetic nanoparticles on surface of conducting fillers results in enhanced network formation at relatively very low fraction of fillers which further leads to maximum total attenuation and absorption of incident EM radiation. This opens up new avenues of decorating GO sheets with Ni rather than Ni nanoparticles for designing cost-effective and lightweight nanocomposites.

Thickness of the shield has vital role in total attenuation of EM radiation. In order to analyze the effect of thickness, SE total was studied at different specimen thicknesses for few blends. The skin depth of PE/PEO blends with MWNTs and Ni was observed to be 4 mm. To neglect the multiple reflections, specimen thickness selected (6 mm) was well above the skin depth although samples with different thickness has been studied to gain in depth understanding of the effect of thickness of SE Figure 8 depicts SE total as a function of frequency and thickness for blends with Ni and GO-Ni nanoparticles, respectively. It is evident that SE total scales with thickness and it is comprehensively evident in both the blends. From the various studies, it is evident that absorption of EM radiation scales with thickness. Similar observation was evident in PE/PEO blends where the total shielding effectiveness increased with the thickness of specimen and this could be ascribed to enhanced absorption of EM radiation.

Mechanism of Attenuation in PE/PEO Blends Composites. To obtain more insight about attenuation mechanisms the relative permittivity and permeability of blends were studied in a broad frequency range. It is well-known that owing to their electrical dipoles MWNTs can be used to tailor permittivity whereas presence of magnetic fillers can tailor the permeability of composites. The presence of both electrical and magnetic dipoles plays important role in absorption of EM radiation in

DOI: 10.1021/acsami.5b02703
ACS Appl. Mater. Interfaces 2015, 7, 16266−16278

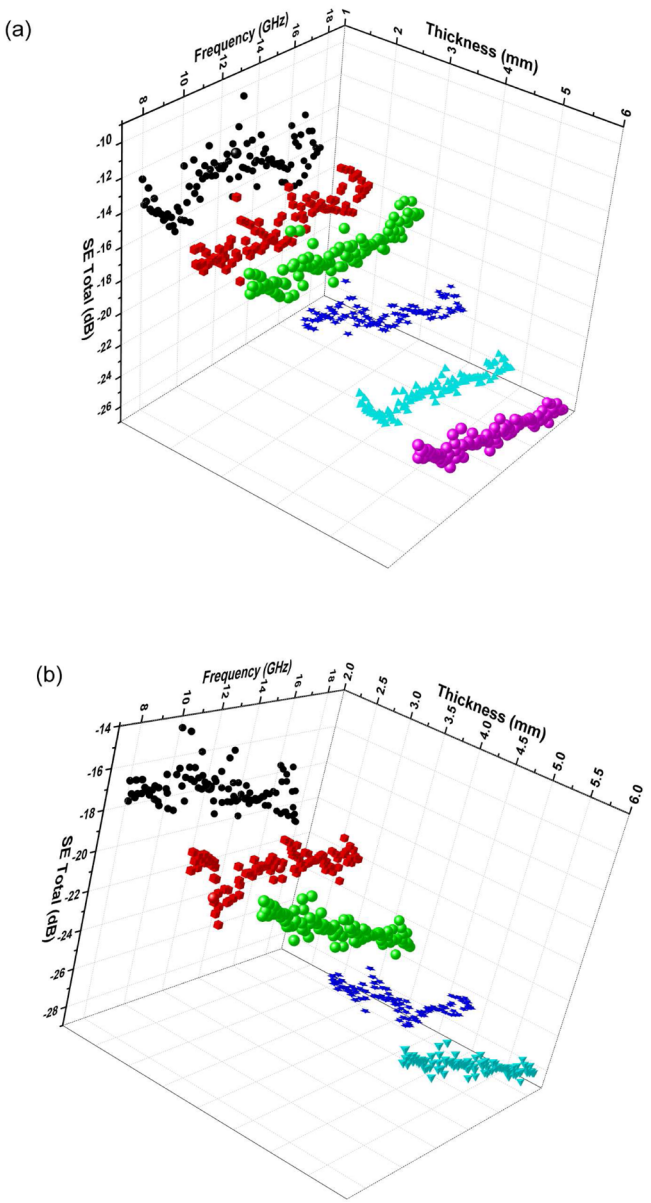

Figure 8. Total shielding effectiveness as a function of frequency and thickness for 70/30 PE/PEO with (a) 10 vol % Ni and (b) GO-Ni.

polymer nanocomposites. Here, by assistance with MWNTs and Ni nanoparticles, we could able to design soft nanocomposites with enhanced permittivity and permeability. Relative permittivity and permeability was estimated using well established line theory using scattering parameters extracted from vector network analyzer (VNA).

The SE_R corresponds to the total reflected EM radiation from the surface of shield whereas the RL (reflection loss) represents the maximum absorption of EM waves at particular frequency due to change in complex microwave properties like relative permittivity and permeability of the shield. The SE_R shows contribution of reflection mechanism in total attenuation of microwave radiation and is characteristic of conducting shield. The higher electrical conductivity enhances the both absorption (SE_A) and reflection (SE_R) and eventually leads to maximum total microwave attenuation, whereas, RL can be enhanced by higher value of permittivity and permeability. The SE_R, SE_A, and RL combined provide clear understanding of shield material in the wide frequency range.

In case of air filled coaxial line, the reflection coefficient of EM wave incident on the interface can be expressed as follows:

$$\Gamma = \frac{Z - Z_0}{Z + Z_0} = \frac{(\sqrt{\mu_R/\varepsilon_R} - 1)}{(\sqrt{\mu_R/\varepsilon_R} + 1)} \tag{3}$$

In case of specimen with particular thickness t, the transmission coefficient across the specimen thickness may be expressed as follows:

$$z = e^{-j\omega\sqrt{\mu\varepsilon}\,t} = e^{(-j(\omega/c)\sqrt{\mu_R\varepsilon_R}\,t)} \tag{4}$$

ε_R and μ_R can be complex permittivity and permeability, respectively. Z_0 is characteristic impedance corresponding to coaxial line, and Z is new characteristic impedance of specimen mounting region.

Scattering parameters were obtained from vector network analyzer (VNA) using coaxial setup and their sum and difference are mentioned below.

$$V_1 = S_{21} + S_{11} \tag{5}$$

$$V_2 = S_{21} - S_{11} \tag{6}$$

where S_{11} and S_{21} is the forward reflection coefficient and forward transmission coefficient, respectively.

Reflection coefficient may be estimated using scattering parameters

$$\Gamma = X \pm \sqrt{X^2 - 1} \tag{7}$$

where

$$X = \frac{1 - V_1V_2}{V_1 - V_2} \tag{8}$$

and condition of $|\Gamma| \leq 1$ was satisfied by choosing appropriate sign.

Now, it can be defined as

$$\frac{\mu_R}{\varepsilon_R} = \left[\frac{1 + \Gamma}{1 - \Gamma}\right]^2 = c_1 \tag{9}$$

$$\mu_R\varepsilon_R = -\left[\frac{c}{\omega t}\ln\left(\frac{1}{z}\right)\right]^2 = c_2 \tag{10}$$

The complex permeability and permittivity may be expressed as

$$\mu_R = \sqrt{c_1c_2} \tag{11}$$

$$\varepsilon_R = \sqrt{\frac{c_1}{c_2}} \tag{12}$$

Figure 9 depicts the change of relative permittivity and permeability of blends with frequency. The effect of individual fillers on permittivity and permeability is systematically interpreted in Figure 9. EM radiations consist of electric and magnetic fields. In order to attenuate both the fields, materials should possess electrical conductivity, dielectric, and magnetic dipoles. The presence of MWNTs and GO in PE/PEO blends manifests electrical conductivity and electrical dipole that results in reflection and absorption of electrical field. However, MWNT and graphene oxide are nonmagnetic in nature thus transparent to magnetic field associated with EM radiations. To attenuate the magnetic field, Ni nanoparticles were introduced in the blends. In this context, blends with 3 wt % MWNTs and

DOI: 10.1021/acsami.5b02703
ACS Appl. Mater. Interfaces 2015, 7, 16266−16278

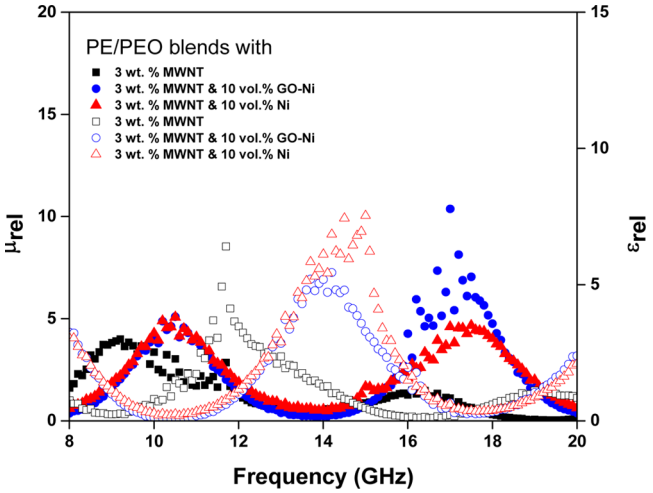

Figure 9. Relative permittivity and permeability as a function of frequency for 70/30 PE/PEO blends (open symbols indicate the permittivity and the closed symbols indicate permeability values).

10 vol % GO-Ni manifested highest permeability which confirms the presence of magnetic dipoles in system that can further interact with an incident EM radiation. The combined effect is due to electrical dipoles in MWNTs and GO and magnetic dipoles in Ni nanoparticles, which led to the highest attenuation of EM radiation through absorption of electrical and magnetic field respectively, in the PE/PEO blends. Because of its electrical dipoles, MWNTs imparted permittivity to composites, where addition of Ni or GO-Ni manifested no effect on relative permittivity of composites. However, interestingly, addition of Ni and GO-Ni imparted striking enhancement in permeability over blends with only MWNTs. This observation supports the combined effect of MWNTs and Ni nanoparticles in absorption of EM radiation where electrical and magnetic dipoles interact with incident EM radiation. These mechanisms of attenuations were further analyzed using different EM parameters like reflection loss (RL), shielding effectiveness through reflection (SE_R) and absorption (SE_A).

The RL can be calculated from relative permeability and permittivity estimated using well adopted line theory by following relation:

$$RL = 20 \times \log \frac{|Z_{in} - 1|}{|Z_{in} + 1|} \quad (13)$$

Figure 10a shows RL as a function of frequency for different blends. Blends with MWNTs depicted RL of −6 dB at 16.4 GHz. Interestingly, blends with 10 vol % Ni and GO-Ni manifested minimum RL of −38.2 and −41 dB at 4.5 and 14.9 GHz, respectively. These minimum reflection losses at particular frequencies correspond to the synergetic absorption of both electrical and magnetic fields associated with EM radiation. The thickness of shield has prominent effect on attenuation of EM radiations. In order to study the effect of shield thickness, RL was analyzes as a function of thickness over broadband frequency range for few blends. Figures 10b and c depict reflection loss as a function of thickness and frequency for blends with Ni and GO-Ni, respectively. It was observed that frequency at which minimum reflection achieved was altered with variation in shield thickness. In case of blends with Ni nanoparticles (Figure 10b), the minimum reflection loss was shifted to higher frequencies with increasing thickness of shield

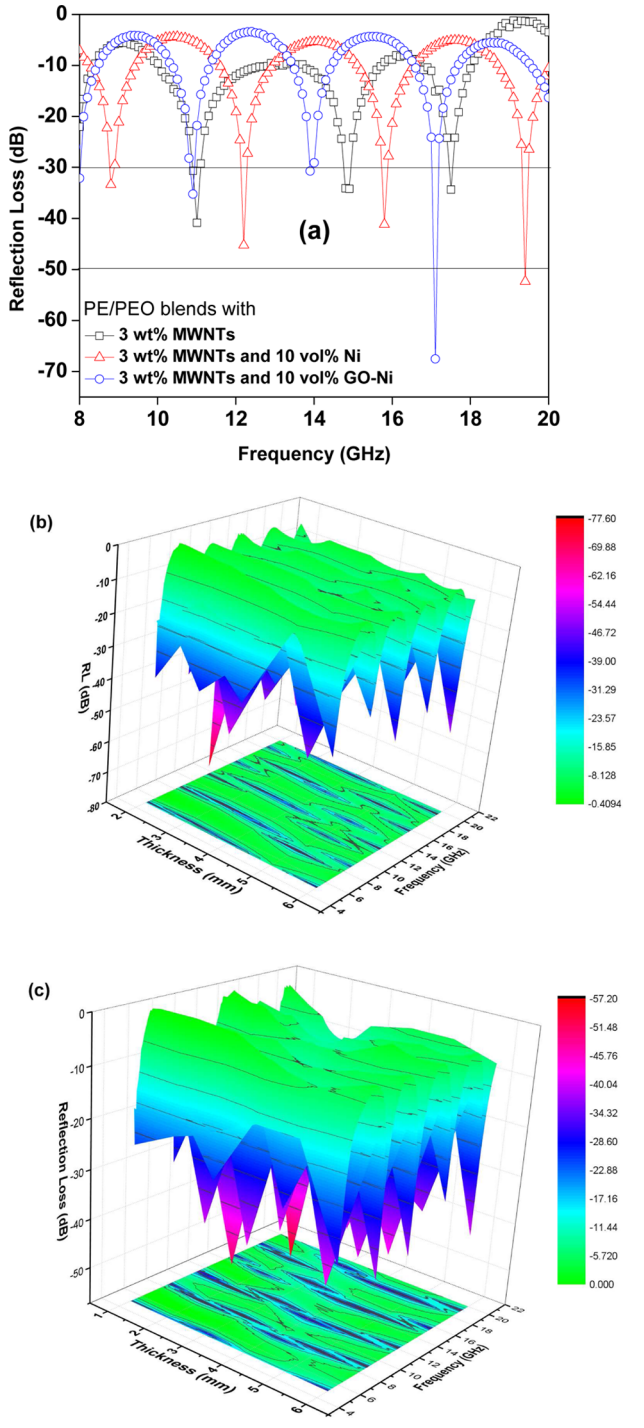

Figure 10. (a) Reflection loss (RL) dependence on the frequency of blends for 6 mm thick specimen, and RL as a function of frequency and thickness for blends with (b) Ni nanoparticles and (c) GO-Ni.

in the X and Ku-band. However, the bandwidth was unaltered. A similar trend was exhibited by blends with GO-Ni (Figure 10c). This suggests appropriate choice of shield thickness for particular application at different frequency ranges. These observations provide insights for designing the shield for specific frequencies.

The contribution of reflection and absorption mechanisms toward attenuation was further estimated using

DOI: 10.1021/acsami.5b02703
ACS Appl. Mater. Interfaces 2015, 7, 16266−16278

$$SE_R\ (dB) = 10 \times \log\left[\frac{1}{(1 - S_{12}{}^2)}\right] \quad (14)$$

$$SE_A\ (dB) = 10 \times \log\left[\frac{(1 - S_{11}{}^2)}{(S_{12}{}^2)}\right] \quad (15)$$

where S_{11} is forward reflection coefficient, S_{12} is reverse transmission coefficient, and S_{21} is forward transmission coefficient. Generally SE_{MR} mechanism have deteriorative effect on SE moreover when is more than 15 dB SE_{MR}.[49]

Figure 11 demonstrates the contribution of SE_A and SE_R toward total EM attenuation for different blends studied here.

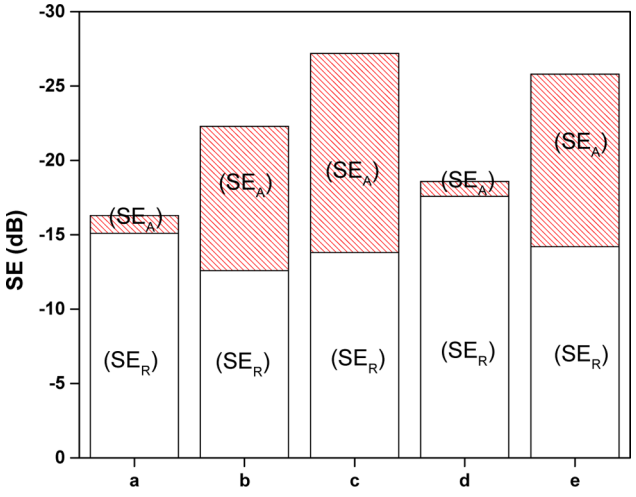

Figure 11. Absorption and reflection components of the total SE at 18 GHz frequency for the blends containing (a) 3 wt % MWNT, (b) 3 wt % MWNT and 5 vol % Ni, (c) 3 wt % MWNT and 10 vol % Ni, (d) 3 wt % MWNT and 5 vol % GO-Ni, and (e) 3 wt % MWNT and 10 vol % GO-Ni.

From contribution of reflection and absorption, it is evident that blends with only MWNTs depicted attenuation mostly through reflection whereas addition of magnetic Ni nanoparticles resulted in enhanced absorption. It is observed that 70/30 PE/PEO with 3 wt % MWNT exhibit a SE_T of −16 dB, which is primarily through reflection. But with the addition of 5 (34 wt %) and 10 vol % (52 wt %) Ni nanoparticles, SE_T was observed to enhance significantly in contrast to MWNTs, which could be attributed to network formation of MWNTs assisted by Ni nanoparticles. As shown in Figure 4b, the PE/PEO blends with 3 wt % MWNTs showed AC electrical conductivity of 10^{-6} S/cm, whereas further incorporation of Ni nanoparticles resulted in enhanced electrical conductivity. This observation supports Ni nanoparticles assisted network formation of MWNTs in the blends.

Interestingly, blends with 5 vol % Ni nanoparticles absorption was enhanced to −9.7 dB in contrast with blends with MWNTs which manifested negligible absorption. Attenuation through absorption was further enhanced by increasing the fraction of Ni nanoparticles where blends containing 10 vol % Ni nanoparticles showed absorption of −13.4 dB. This observation could be ascribed to synergetic absorption of electrical field through MWNTs and magnetic field by Ni nanoparticles consisting of magnetic dipoles. In order to attenuate EM radiation by absorption, the material should be conducting but very high electrical conductivity is not required. However, to achieve electrical conductivity, a connecting network of conducting filler is required.[26] In order to further enhance dispersion and network formation between MWNTs and magnetic particles, Ni nanoparticles were decorated on GO surface. Interestingly, synergetic network of conducting MWNTs and GO-Ni was formed, which is evident from enhanced DC conductivity over only MWNTs. It is important to note that Ni and GO-Ni nanoparticles also are part of resulted network and enhanced dispersion, which resulted in maximum attenuation of EM radiation through absorption at very low weight fraction of fillers. Interestingly, mechanism of attenuation was observed to shift from reflection to absorption for blends with 10 vol % Ni nanoparticles.

The contribution of SE through absorption scaled with concentration of Ni nanoparticles. This can be supported through enhanced permeability of blends with addition of Ni nanoparticles. In case of blends with 3 wt % MWNTs and 5 vol % Ni, magnetic dipoles are not sufficient to absorb maximum magnetic field. In order to study the mechanism, SE through absorption was evaluated. From Figure 11, it is evident that blends with 3 wt % MWNTs and 5 vol % Ni showed maximum attenuation through reflection whereas, blends with 3 wt % MWNTs and 10 vol % Ni manifested 50% SE through absorption. This clearly indicates that with increasing fraction of Ni nanoparticles, absorption is the dominating mechanism for the attenuation of EM radiation.

A similar trend was observed in blends with GO-Ni where SE and absorption scales with fraction of GO-Ni. The effect of enhanced network formation in case of blends with GO-Ni is significantly evident here where total SE and attenuation through absorption is comparable to blends with Ni at relatively very small weight fraction of magnetic filler. The use of very high surface area GO nanoparticles as a substrate to decorate Ni nanoparticles turns out to be a very efficient strategy to achieve enhanced EM attenuation through absorption at very small weight fraction of filler loading. Thus, this opens up new avenues of decorating GO sheets with magnetic nanoparticles rather than physical mixing of magnetic nanoparticles for effective cost and weight saving.

CONCLUSIONS

EMI shielding of PE/PEO blends with MWNT, Ni, and GO-Ni were assessed in a broad range of frequencies. The synthesis of Ni and GO-Ni particles was well characterized by XRD, XPS, TEM, SEM, and FTIR. The addition of Ni and GO-Ni along with MWNT enhanced the electrical conductivity of the blends significantly. The addition of Ni decorated MWNT led to increase in contact resistance, whereas GO-Ni facilitated the network-like structure of MWNTs and hence, resulted in significantly high electrical conductivity. Further, GO-Ni (with effective concentration of Ni as 19 wt %) exhibited a conductivity of $\sim 10^{-4}$ S·cm^{-1}, which is similar to the blends containing Ni and MWNTs (where the effective concentration of Ni is 52 wt %). The blends containing 3 wt % MWNTs and 10 vol % Ni (52 wt %) exhibited a SE_T of −27 dB, whereas similar SE was obtained for the combination of GO-Ni and MWNTs. However, in the latter case the effective concentration of Ni was 2.7 times lower. More interestingly, blends with MWNTs/GO-Ni showed a minimum reflection loss of −70 dB for a 6 mm thick shield at 17.1 GHz frequency and blocked the incoming radiations mostly by absorption. This study opens new avenues in designing polyolefin based

DOI: 10.1021/acsami.5b02703
ACS Appl. Mater. Interfaces 2015, 7, 16266−16278

lightweight shielding materials by engineering nanostructures for numerous applications.

AUTHOR INFORMATION

Corresponding Author

*E-mail: sbose@materials.iisc.ernet.in.

Notes

The authors declare no competing financial interest.

ACKNOWLEDGMENTS

We thank Department of Science and Technology (DSTO1150) for the financial support. We would like to thank MNCF, AFMM for extending characterization facilities.

REFERENCES

(1) Chandrasekhar, P.; Naishadham, K. Broadband Microwave Absorption and Shielding Properties of a Poly(Aniline). *Synth. Met.* **1999**, *105*, 115−120.

(2) Kim, M. S.; Kim, H. K.; Byun, S. W.; Jeong, S. H.; Hong, Y. K.; Joo, J. S.; Song, K. T.; Kim, J. K.; Lee, C. J.; Lee, J. Y. Pet Fabric/Polypyrrole Composite with High Electrical Conductivity for EMI Shielding. *Synth. Met.* **2002**, *126*, 233−239.

(3) Sienkiewicz, Z. Biological Effects of Electromagnetic Fields. *Power Eng. J.* **1998**, *12*, 131−139.

(4) Sharma, M.; Sharma, S.; Abraham, J.; Thomas, S.; Madras, G.; Bose, S. Flexible EMI Shielding Materials Derived by Melt Blending PVDF and Ionic Liquid Modified MWNTs. *Mater. Res. Express* **2014**, *1*, 035003.

(5) Sharma, M.; Singh, M. P.; Srivastava, C.; Madras, G.; Bose, S. Poly(Vinylidene Fluoride)-Based Flexible and Lightweight Materials for Attenuating Microwave Radiations. *ACS Appl. Mater. Interfaces* **2014**, *6*, 21151−21160.

(6) Pawar, S. P.; Pattabhi, K.; Bose, S. Assessing the Critical Concentration of NH_2 Terminal Groups on the Surface of MWNTs Towards Chain Scission of PC in PC/SAN Blends: Effect on Dispersion, Electrical Conductivity and EMI Shielding. *RSC Adv.* **2014**, *4*, 18842−18852.

(7) Pawar, S. P.; Marathe, D. A.; Pattabhi, K.; Bose, S. Electromagnetic Interference Shielding through MWNT Grafted Fe_3O_4 Nanoparticles in PC/SAN Blends. *J. Mater. Chem. A* **2015**, *3*, 656−669.

(8) Xavier, P.; Bose, S. Electromagnetic Shielding Materials and Coatings Derived from Gelation of Multiwall Carbon Nanotubes in an LCST Mixture. *RSC Adv.* **2014**, *4*, 55341−55348.

(9) Rohini, R.; Bose, S. Electromagnetic Interference Shielding Materials Derived from Gelation of Multiwall Carbon Nanotubes in Polystyrene/Poly(Methyl Methacrylate) Blends. *ACS Appl. Mater. Interfaces* **2014**, *6*, 11302−11310.

(10) Bose, S.; Khare, R. A.; Moldenaers, P. Assessing the Strengths and Weaknesses of Various Types of Pre-Treatments of Carbon Nanotubes on the Properties of Polymer/Carbon Nanotubes Composites: A Critical Review. *Polymer* **2010**, *51*, 975−993.

(11) Utracki, L. A. *Polymer Blends Handbook*; Kluwer Academic Publishers; Dordrecht, The Netherlands, 2002; Chapter 1, pp 13.

(12) Ryu, D. Y.; Lee, D. H.; Jang, J.; Kim, J. K.; Lavery, K. A.; Russell, T. P. Complex Phase Behavior of a Weakly Interacting Binary Polymer Blend. *Macromolecules* **2004**, *37*, 5851−5855.

(13) Bose, S.; Bhattacharyya, A. R.; Kulkarni, A. R.; Pötschke, P. Electrical, Rheological and Morphological Studies in Co-Continuous Blends of Polyamide 6 and Acrylonitrile−Butadiene−Styrene with Multiwall Carbon Nanotubes Prepared by Melt Blending. *Compos. Sci. Technol.* **2009**, *69*, 365−372.

(14) Mural, P. K. S.; Madras, G.; Bose, S. Positive Temperature Coefficient and Structural Relaxations in Selectively Localized Mwnts in PE/PEO Blends. *RSC Adv.* **2014**, *4*, 4943−4954.

(15) Mural, P. K. S.; Rana, M. S.; Madras, G.; Bose, S. PE/PEO Blends Compatibilized by PE Brush Immobilized on MWNTs: Improved Interfacial and Structural Properties. *RSC Adv.* **2014**, *4*, 16250−16259.

(16) Singh, B. P.; Prabha; Saini, P.; Gupta, T.; Garg, P.; Kumar, G.; Pande, I.; Pande, S.; Seth, R. K.; Dhawan, S. K.; Mathur, R. B. Designing of Multiwalled Carbon Nanotubes Reinforced Low Density Polyethylene Nanocomposites for Suppression of Electromagnetic Radiation. *J. Nanopart. Res.* **2011**, *13*, 7065−7074.

(17) Al-Saleh, M. H.; Sundararaj, U. Electromagnetic Interference Shielding Mechanisms of Cnt/Polymer Composites. *Carbon* **2009**, *47*, 1738−1746.

(18) Yang, Y.; Gupta, M. C.; Dudley, K. L.; Lawrence, R. W. Novel Carbon Nanotube−Polystyrene Foam Composites for Electromagnetic Interference Shielding. *Nano Lett.* **2005**, *5*, 2131−2134.

(19) Hoang, A. S. Electrical Conductivity and Electromagnetic Interference Shielding Characteristics of Multiwalled Carbon Nanotube Filled Polyurethane Composite Films. *Adv. Nat. Sci.: Nanosci. Nanotechnol.* **2011**, *2*, 025007.

(20) Huang, Y.; Li, N.; Ma, Y.; Du, F.; Li, F.; He, X.; Lin, X.; Gao, H.; Chen, Y. The Influence of Single-Walled Carbon Nanotube Structure on the Electromagnetic Interference Shielding Efficiency of Its Epoxy Composites. *Carbon* **2007**, *45*, 1614−1621.

(21) Liang, J.; Wang, Y.; Huang, Y.; Ma, Y.; Liu, Z.; Cai, J.; Zhang, C.; Gao, H.; Chen, Y. Electromagnetic Interference Shielding of Graphene/Epoxy Composites. *Carbon* **2009**, *47*, 922−925.

(22) Maiti, S.; Suin, S.; Shrivastava, N. K.; Khatua, B. B. A Strategy to Achieve High Electromagnetic Interference Shielding and Ultra Low Percolation in Multiwall Carbon Nanotube-Polycarbonate Composites through Selective Localization of Carbon Nanotubes. *RSC Adv.* **2014**, *4*, 7979−7990.

(23) Kim, H. M.; Kim, K.; Lee, C. Y.; Joo, J.; Cho, S. J.; Yoon, H. S.; Pejaković, D. A.; Yoo, J. W.; Epstein, A. J. Electrical Conductivity and Electromagnetic Interference Shielding of Multiwalled Carbon Nanotube Composites Containing Fe Catalyst. *Appl. Phys. Lett.* **2004**, *84*, 589−591.

(24) Kar, G. P.; Biswas, S.; Rohini, R.; Bose, S. Tailoring the Dispersion of Multiwall Carbon Nanotubes in Co-Continuous PVDFABS Blends to Design Materials with Enhanced Electromagnetic Interference Shielding. *J. Mater. Chem. A* **2015**, *3*, 7974−7985.

(25) Zhang, Y.; Huang, Y.; Zhang, T.; Chang, H.; Xiao, P.; Chen, H.; Huang, Z.; Chen, Y. Broadband and Tunable High-Performance Microwave Absorption of an Ultralight and Highly Compressible Graphene Foam. *Adv. Mater.* **2015**, *27*, 2049−2053.

(26) Chung, D. Materials for Electromagnetic Interference Shielding. *J. Mater. Eng. Perform.* **2000**, *9*, 350−354.

(27) Mural, P. K. S.; Banerjee, A.; Rana, M. S.; Shukla, A.; Padmanabhan, B.; Bhadra, S.; Madras, G.; Bose, S. Polyolefin Based Antibacterial Membranes Derived from PE/PEO Blends Compatibilized with Amine Terminated Graphene Oxide and Maleated PE. *J. Mater. Chem. A* **2014**, *2*, 17635−17648.

(28) Tang, Y.; Yang, D.; Qin, F.; Hu, J.; Wang, C.; Xu, H. Decorating Multi-Walled Carbon Nanotubes with Nickel Nanoparticles for Selective Hydrogenation of Citral. *J. Solid State Chem.* **2009**, *182*, 2279−2284.

(29) Kim, H.-S.; Lee, H.; Han, K.-S.; Kim, J.-H.; Song, M.-S.; Park, M.-S.; Lee, J.-Y.; Kang, J.-K. Hydrogen Storage in Ni Nanoparticle-Dispersed Multiwalled Carbon Nanotubes. *J. Phys. Chem. B* **2005**, *109*, 8983−8986.

(30) Arai, S.; Endo, M.; Kaneko, N. Ni-Deposited Multi-Walled Carbon Nanotubes by Electrodeposition. *Carbon* **2004**, *42*, 641−644.

(31) Hu, X.; Dong, S. Metal Nanomaterials and Carbon Nanotubes-Synthesis, Functionalization and Potential Applications Towards Electrochemistry. *J. Mater. Chem.* **2008**, *18*, 1279−1295.

(32) Hull, R. V.; Li, L.; Xing, Y.; Chusuei, C. C. Pt Nanoparticle Binding on Functionalized Multiwalled Carbon Nanotubes. *Chem. Mater.* **2006**, *18*, 1780−1788.

(33) Yu, R.; Chen, L.; Liu, Q.; Lin, J.; Tan, K.-L.; Ng, S. C.; Chan, H. S. O.; Xu, G.-Q.; Hor, T. S. A. Platinum Deposition on Carbon Nanotubes Via Chemical Modification. *Chem. Mater.* **1998**, *10*, 718−722.

DOI: 10.1021/acsami.5b02703
ACS Appl. Mater. Interfaces 2015, 7, 16266−16278

(34) Niyogi, S.; Hamon, M. A.; Hu, H.; Zhao, B.; Bhowmik, P.; Sen, R.; Itkis, M. E.; Haddon, R. C. Chemistry of Single-Walled Carbon Nanotubes. *Acc. Chem. Res.* **2002**, *35*, 1105−1113.
(35) Tasis, D.; Tagmatarchis, N.; Bianco, A.; Prato, M. Chemistry of Carbon Nanotubes. *Chem. Rev.* **2006**, *106*, 1105−1136.
(36) Guo, G.; Qin, F.; Yang, D.; Wang, C.; Xu, H.; Yang, S. Synthesis of Platinum Nanoparticles Supported on Poly(Acrylic Acid) Grafted MWNT and Their Hydrogenation of Citral. *Chem. Mater.* **2008**, *20*, 2291−2297.
(37) Davar, F.; Fereshteh, Z.; Salavati-Niasari, M. Nanoparticles Ni and NiO: Synthesis, Characterization and Magnetic Properties. *J. Alloys Compd.* **2009**, *476*, 797−801.
(38) Gupta, V.; Saleh, T. A. *Syntheses of Carbon Nanotube−Metal Oxides Composites: Adsorption and Photo-Degradation*; INTECH Open Access Publisher: Rijeka, Croatia, 2011.
(39) Park, H.-S.; Gong, M.-S. Facile Preparation of Nanosilver-Decorated MWNT Using Silver Carbamate Complex and Their Polymer Composites. *Bull. Korean Chem. Soc.* **2012**, *33*, 483−488.
(40) Hummers, W. S., Jr; Offeman, R. E. Preparation of Graphitic Oxide. *J. Am. Chem. Soc.* **1958**, *80*, 1339−1339.
(41) Kumar, S.; Chatterjee, K. Strontium Eluting Graphene Hybrid Nanoparticles Augment Osteogenesis in a 3D Tissue Scaffold. *Nanoscale* **2015**, *7*, 2023−2033.
(42) Ji, Z.; Shen, X.; Zhu, G.; Zhou, H.; Yuan, A. Reduced Graphene Oxide/Nickel Nanocomposites: Facile Synthesis, Magnetic and Catalytic Properties. *J. Mater. Chem.* **2012**, *22*, 3471−3477.
(43) Sumita, M.; Sakata, K.; Hayakawa, Y.; Asai, S.; Miyasaka, K.; Tanemura, M. Double Percolation Effect on the Electrical Conductivity of Conductive Particles Filled Polymer Blends. *Colloid Polym. Sci.* **1992**, *270*, 134−139.
(44) Mural, P. K.; Mohanty, S.; Nayak, S. K.; Anbudayanidhi, S. Polypropylene/High Impact Polystyrene Blend Nanocomposites Obtained from E-Waste: Evaluation of Mechanical, Thermal and Morphological Properties. *Int. J. Plast. Technol.* **2011**, *15*, 46−60.
(45) Liang, G. D.; Tjong, S. C. Electrical Properties of Low-Density Polyethylene/Multiwalled Carbon Nanotube Nanocomposites. *Mater. Chem. Phys.* **2006**, *100*, 132−137.
(46) Ryu, S.; Mo, C. B.; Lee, H.; Hong, S. H. Fabrication Process and Electromagnetic Wave Absorption Characterization of a CNT/Ni/Epoxy Nanocomposite. *J. Nanosci. Nanotechnol.* **2013**, *13*, 7669−7674.
(47) He, X.; Zhong, W.; Au, C.-T.; Du, Y. Size Dependence of the Magnetic Properties of Ni Nanoparticles Prepared by Thermal Decomposition Method. *Nanoscale Res. Lett.* **2013**, *8*, 446.
(48) Abbas, S.; Dixit, A.; Chatterjee, R.; Goel, T. Complex Permittivity, Complex Permeability and Microwave Absorption Properties of Ferrite−Polymer Composites. *J. Magn. Magn. Mater.* **2007**, *309*, 20−24.
(49) Li, N.; Huang, Y.; Du, F.; He, X.; Lin, X.; Gao, H.; Ma, Y.; Li, F.; Chen, Y.; Eklund, P. C. Electromagnetic Interference (EMI) Shielding of Single-Walled Carbon Nanotube Epoxy Composites. *Nano Lett.* **2006**, *6*, 1141−1145.

DOI: 10.1021/acsami.5b02703
ACS Appl. Mater. Interfaces 2015, 7, 16266−16278